ENSO diversity in climate models

Antonietta Capotondi[1] and Andrew Wittenberg[2]
[1]NOAA/Earth System Research Laboratory
[2]NOAA/Geophysical Fluid Dynamics Laboratory

Understanding the nature of El Niño – Southern Oscillation (ENSO) diversity in observations is challenging. Due to the relatively short duration of the observational record and the sparsity of subsurface data, it is difficult to characterize different ENSO flavors, and understand their underlying dynamics, triggers, and impacts, with high statistical confidence (Vecchi and Wittenberg 2010).

Climate models can help overcome these limitations by providing long global time series of relevant physical quantities, with detailed and self-consistent surface and subsurface information. Climate model simulations exist for pre-industrial and historical periods, as well as for different climate change scenarios -- thus allowing characterization of ENSO diversity both in the context of natural variability and in the presence of anthropogenic forcing. However, climate models have biases in their ENSO simulation (as well as mean state), including amplitude, spatial pattern, spectral characteristics, and

leading dynamical processes – as documented in studies that have examined the World Climate Research Program Climate Model Intercomparison Project (CMIP) phases 3 and 5 archives (Capotondi et al. 2006; Guilyardi et al. 2009; Delworth et al. 2012; Watanabe and Wittenberg 2012; Watanabe et al. 2012).

How well do climate models simulate ENSO diversity? One important aspect is the ability to represent events that differ in the amplitude and longitude of peak tropical Pacific sea surface temperature anomalies (SSTAs). Various diagnostic approaches have been proposed to characterize the longitudinal diversity. Following Kug et al. (2009), we focus on the warm ENSO phase and use SSTA averages over the Niño3 (eastern equatorial Pacific, 150˚W-90˚W, 5˚S-5˚N) and Niño4 (western/central equatorial Pacific, 160˚E-150˚W, 5˚S-5˚N) regions to stratify events by longitude. We refer to events with peak SSTAs in Niño3 as "Cold Tongue" (CT) events, and those with peak SSTAs in Niño4 as "Warm Pool" (WP) events.
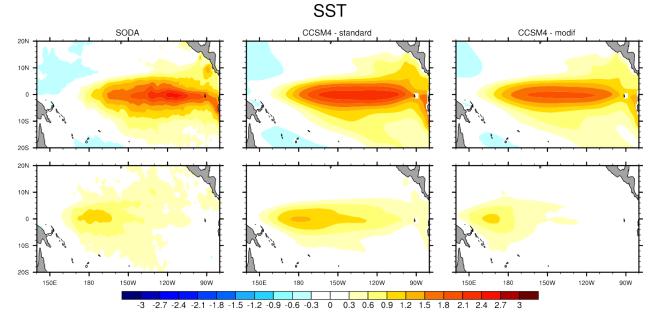

Figure 1. Composite SSTA patterns for SODA (left panels), CCSM4 (middle panels), and CCSM4 with modified indices (right panels). CT events are shown on the top row, and WP events in the bottom row. Units are °C. CT events are identified by requiring that the winter (JFM) Niño3 index is larger than 0.5°C and larger than the Niño4 index, and vice versa for WP events.

Climate models are characterized by SSTAs extending farther west than observed (Capotondi et al. 2006), and this bias may limit the models' ability to simulate events that peak at diverse longitudes. As a result, only a relatively small subset of the CMIP3 archive exhibits clearly distinguishable CT and WP extremes (Kug et al. 2010; Ham and Kug 2012), and several models show a large overlap between patterns of warming associated with the CT and WP events. Similarly, only a few models in the CMIP3 ensemble produce a realistic intensity ratio for the two El Niño types (Yu and Kim 2010).

Some models, however, do produce a rich spectrum of ENSO diversity, with characteristics similar to those

observed. In this article, we show results from two climate models participating in the CMIP5: the National Center for Atmospheric Research Community Climate System Model version 4 (NCAR-CCSM4), and the Geophysical Fluid Dynamics Laboratory Climate Model version 2.1 (GFDL-CM2.1). Fig. 1 shows the spatial patterns of SSTAs, in a composite sense, for CT (top panels) and WP (lower panels) events in the Simple Ocean Data Assimilation (SODA) version 2.0.2/3 (left panels), and in the NCAR-CCSM4 (middle and right panels). This version of SODA covers the period 1958-2007, while the model results are based upon a 500-year pre-industrial control simulation. Modified indices – displaced 20° to the west of the standard Niño3 and Niño4, and defined here as Niño3-m and Niño4-m – are also examined to account for the model's tendency to displace its SSTAs west of the observed patterns. While this model bias is not very pronounced in the NCAR-CCSM4, the use of both standard and modified indices allows the identification of events whose anomalies peak at different longitudes. The relatively good agreement between SODA and the NCAR-CCSM4 is an indication of the model's ability to simulate different ENSO flavors.

The dynamical processes associated with El Niño diversity in the NCAR-CCSM4 and GFDL-CM2.1 are also consistent with those found in observational studies (Kug et al. 2009). A heat budget analysis performed over the Niño3, Niño3-m, Niño4 and Niño4-m regions in NCAR-CCSM4 (Fig. 2) shows that ocean dynamical processes, in particular vertical and horizontal advection, play a key role in both the development and decay of warm events in the eastern Pacific, while in the central/western Pacific the decay of warm events is primarily due to the damping effect of the surface heat flux. Because the thermocline is shallower in the eastern than in the western Pacific, vertical
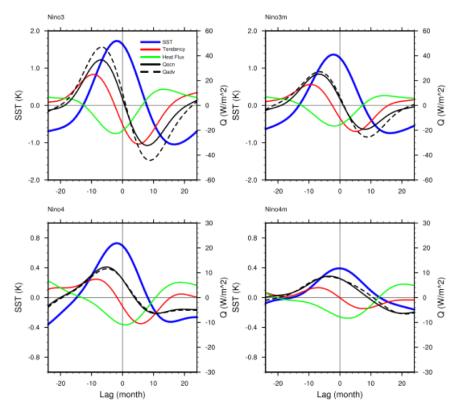

Figure 2. Composite evolution of the different heat budget terms (right y-axis) averaged over the Niño3 (top-left), Niño3-m (top-right), Niño4 (bottom-left), and Niño4-m (bottom-right) regions, and to 65m depth. For this analysis the regions extend meridionally from 2.5°S to 2.5°N, to better characterize processes that are confined near the equator, like upwelling. In each region, the composite is computed over the events peaking in that region. The SSTA evolution (thick blue curve, left y-axis) in each region is also shown for comparison. Lag 0 corresponds to the January of the event peak (events are identified by the DJF SSTA), and the evolution of each quantity is shown over a 48-month period. The black solid line shows the oceanic heat flux convergence (Q_{ocn}), computed as a residual between the tendency term (red line) and the surface heat flux (green line), while the black dashed line shows the oceanic advection term (Q_{adv}), diagnosed directly from the ocean model fields.

advection processes are relatively more important in the evolution of eastern Pacific events, while zonal advection plays a key role in the growth of central/western Pacific events (not shown). The results for the NCAR-CCSM4 model are qualitatively similar to those obtained from the GFDL-CM2.1 model (Kug et al. 2010). Differences are found between the two models in the relative frequency of CT vs. WP cases, as well as in the exact role of different advection processes. A broader community effort toward model intercomparisons is needed to distinguish aspects of ENSO diversity that are robust from those that are model-dependent.

A key question regarding ENSO diversity is whether there is a clear bimodality with distinct ENSO types, or rather a broad continuum with interesting extremes.

The short duration of the instrumental record is problematic for answering this question. Multi-proxy paleoreconstructions (e.g. Li et al. 2011; Emile-Geay et al. 2013a,b; McGregor et al. 2013) may eventually provide reliable longer records of ENSO, though these efforts are still in their infancy. Meanwhile, long model simulations can provide valuable insights. For example, a 4000-year pre-industrial control simulation from GFDL CM2.1 captures much of the observed diversity of ENSO, and permits a detailed look at the distribution of the model's ENSO events (Delworth et al. 2006; Wittenberg et al. 2006; Wittenberg 2009). Because this simulation uses unchanging external forcings, its ENSO diversity is entirely intrinsically generated. The CM2.1 simulation exhibits decadal-to-centennial modulation of its ENSO amplitude, period, skewness, spatial pattern, and predictability (Wittenberg 2009; Kug et al. 2010; Karamperidou et al. 2013), which in turn rectify into longer-term changes in the tropical Pacific mean state (Ogata et al. 2013).

The scatterplot in Fig. 3 shows the peak DJF SSTA along the equator -- and the corresponding longitude where that peak occurs -- for every warm event in the 4000 year CM2.1 control simulation. The events with west Pacific SSTA peaks are always weak, and those with central Pacific peaks are always intermediate in strength. The strongest events always peak in the east Pacific, although east Pacific events can exhibit a wide range of amplitudes. While the marginal distribution of peak amplitudes offers no evidence of bimodality, the marginal distribution of peak longitudes does have a weakly bimodal character – with a tendency for SSTAs to peak most frequently near either 160˚E or 115˚W. However, a naive characterization of the simulated warm events as consisting of distinct "western" and "eastern" types is at odds with the bivariate distribution, which instead shows a continuum of events whose peaks shift eastward as they strengthen, plus a small group of weak cold tongue events.

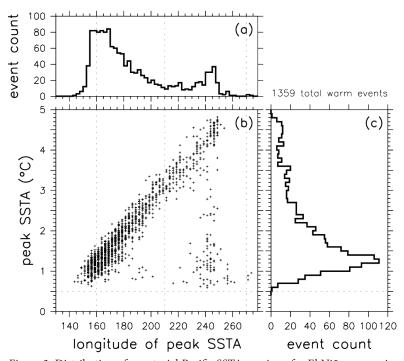One explanation for the triangular-shaped outline of the amplitude vs. longitude

Figure 3: Distribution of equatorial Pacific SSTA maxima, for El Niños occurring in a 4000-year pre industrial control simulation from the GFDL CM2.1 coupled GCM. To qualify as an El Niño, the simulated DJF-mean SSTA averaged over either the Niño3 region (150°W-90°W, 5°-5N) or the Niño4 region (160°E 150°W, 5°S-5°N) must exceed 0.5°C. For each of the 1359 such events, the DJF-mean SSTA is averaged over the equatorial zone (5°S-5°N), and then the Pacific zonal maximum is located. (a) Distribution of peak SSTA longitudes (°E). (b) Scatterplot of the peak SSTA value (°C) versus the longitude (°E) at which it occurs. (c) Distribution of peak SSTA values (°C).

scatterplot in Fig. 3 may be that warming during El Niño is effectively capped at the radiative-convective equilibrium sea surface temperatures (SSTs) of the Indo-Pacific warm pool. The western equatorial Pacific, which is already near these values, has little room for additional warming. East Pacific events, however, can exhibit a wider range of strengths due to the much larger climatological difference between the local SST and the warm pool SST. Strong El Niños may produce more flattening of the equatorial thermocline, boosting vertical advective warming in the east at the expense of the west, and causing the peak warming for such events to appear in the east. Weak El Niños, in contrast, may fail to ignite such basin-wide coupled feedbacks.

One mysterious feature of Fig. 3 is the "hole" in the scatterplot triangle, indicating that moderate, central Pacific events never occur in the model. Perhaps the central Pacific is too far from the strong zonal SST gradients of the west, or the strong vertical temperature gradients of the east, to compete with the SSTAs generated at those locations. Or perhaps nascent central Pacific SSTAs are pulled westward by zonal advective feedbacks or eastward by thermocline feedbacks, causing such events to ultimately present their peak SSTAs in a different location. Further analyses are needed to understand the distributions and life cycles of these diverse events.

By providing long time series as well as platforms for perturbation experiments, CGCMs are helping to illuminate ENSO's teleconnections and impacts (Lee, this volume). As the models become more sophisticated, their simulations of ENSO's teleconnections are improving (e.g., Delworth et al. 2012). Besides being important for assessing societal and ecosystem impacts, teleconnections are also crucial for reconstructing pre-instrumental ENSO variability – since proxy recorders of ENSO (such as corals, tree rings, and lake sediments) are often remote from ENSO's centers of action in the tropical Pacific. Recent studies have used models to investigate the influence of ENSO diversity on proxy reconstructions, using simulated "pseudo-proxies" as a baseline against which to evaluate possible impacts of climatic forcings on ENSO (e.g. Emile-Geay et al. 2013a,b; Cobb et al. 2013; McGregor et al. 2013). By providing a global perspective, paleoclimate simulations can also reconcile seemingly conflicting local views seen by individual proxies

(Karamperidou et al., in prep). Together, observations, models, and theory are helping to paint a more complete picture of ENSO's role in the global climate system.

References

Capotondi, A., A. Wittenberg, and S. Masina, 2006: Spatial and temporal structure of tropical Pacific interannual variability in 20th century coupled simulations. Ocean Model., 15, 274-298.

Cobb, K. M., N. Westphal, H. R. Sayani, J. T. Watson, E. Di Lorenzo, H. Cheng, R. L. Edwards, and C. D. Charles, 2013: Highly variable El Niño-Southern Oscillation throughout the Holocene. Science, 339, 67-70, doi:10.1126/science.1228246.

Delworth, T.L. and Co-authors, 2006: GFDL's CM2 global coupled climate models, Part I: Formulation and simulation characteristics. J. Climate, 19, 643-674, doi:10.1175/JCLI3629.1.

Delworth, T. L., A. Rosati, W. Anderson, A. J. Adcroft, V. Balaji, R. Benson, K. Dixon, S. M. Griffies, H.-C. Lee, R. C. Pacanowski, G. A. Vecchi, A. T. Wittenberg, F. Zeng, and R. Zhang, 2012: Simulated climate and climate change in the GFDL CM2.5 high-resolution coupled climate model. J. Climate, 25, 2755-2781, doi:10.1175/JCLI-D-11-00316.1.

Emile-Geay, J., K. Cobb, M. Mann, and A. T. Wittenberg, 2013a: Estimating central equatorial Pacific SST variability over the past millennium. Part 1: Methodology and validation. J. Climate, 26, 2302-2328, doi:10.1175/JCLI-D-11-00510.1.

Emile-Geay, J., K. Cobb, M. Mann, and A. T. Wittenberg, 2013b: Estimating central equatorial Pacific SST variability over the past millennium. Part 2: Reconstructions and uncertainties. J. Climate, 26, 2329-2352, doi:10.1175/JCLI-D-11-00511.1.

Guilyardi, E. and Coauthors, 2009: Understanding El Niño in ocean-atmosphere general circulation models: Progress and challenges. Bull. Amer. Meteor. Soc., 90, 325-340.

Ham, Y.-G., and J.-S. Kug, 2012: How well do current climate models simulate two types of El Niño? Climate Dyn., 39, 383-398, doi:10.1007/s00382-011-1157-3.

Karamperidou, C., M. A. Cane, U. Lall, and A. T. Wittenberg, 2013: Intrinsic modulation of ENSO predictability viewed through a local Lyapunov lens. Climate Dyn., doi:10.1007/s00382-013-1759-z.

Kug, J.-S., F.-F. Jin, and S.-I. An, 2009: Two types of El Niño events: cold tongue El Niño and warm pool El Niño. J. Climate, 22, 1499–1515.

Kug, J.-S., J. Choi, S.-I. An, F.-F. Jin, and A. T. Wittenberg, 2010: Warm pool and cold tongue El Niño events as simulated by the GFDL CM2.1 coupled GCM. J. Climate, 23, 1226-1239, doi:10.1175/2009JCLI3293.1.

Li, J., S.-P. Xie, E. R. Cook, G. Huang, R. D'Arrigo, F. Liu, J. Ma, and X.-T. Zheng, 2011: Interdecadal modulation of El Niño amplitude during the past millennium. Nature Climate Change, 1, 114-118, doi:10.1038/nclimate1086.

McGregor, S., A. Timmermann, M. H. England, O. Elison Timm, and A. T. Wittenberg, 2013: Inferred changes in El Niño-Southern Oscillation variance over the past six centuries. Climate Past. Discuss., 9, 2929-2966, doi:10.5194/cpd-9-2929-2013.

Ogata, T., S.-P. Xie, A. Wittenberg, and D.-Z. Sun, 2013: Interdecadal amplitude modulation of El Niño/Southern Oscillation and its impacts on tropical Pacific decadal variability. J. Climate, doi:10.1175/JCLI-D-12-00415.1.

Vecchi, G. A. and A. T. Wittenberg, 2010: El Niño and our future climate: Where do we stand? Wiley Interdisciplinary Reviews: Climate Change, 1, 260-270, doi:10.1002/wcc.33.

Watanabe, M. and A. T. Wittenberg, 2012: A method for disentangling El Niño-mean state interaction. Geophys. Res. Lett., 39, L14702, doi:10.1029/2012GL052013.

Watanabe, M., J.-S. Kug, F.-F. Jin, M. Collins, M. Ohba, and A. T. Wittenberg, 2012: Uncertainty in the ENSO amplitude change from the past to the future. Geophys. Res. Lett., 39, L20703, doi:10.1029/2012GL053305.

Wittenberg, A. T., A. Rosati, N.-C. Lau, and J. J. Ploshay, 2006: GFDL's CM2 global coupled climate models, Part III: Tropical Pacific climate and ENSO. J. Climate, 19, 698-722, doi:10.1175/JCLI3631.1.

Wittenberg, A. T., 2009: Are historical records sufficient to constrain ENSO simulations? Geophys. Res. Lett., 36, L12702, doi:10.1029/2009GL038710.

Yu, J.-Y. and S. T. Kim, 2010: Identification of Central-Pacific and Eastern-Pacific Types of ENSO in CMIP3 Models Geophys. Res. Lett.,, 37, L15705, doi:10.1029/2010GL044082.

Extra-tropical precursors of ENSO flavors

Emanuele Di Lorenzo[1], Honghai Zhang[2], Amy Clement[2], Bruce Anderson[3], and Alexey Fedorov[4]
[1]School of Earth and Atmospheric Sciences, Georgia Institute of Technology
[2]Rosenstiel School of Marine and Atmospheric Science, University of Miami
[3]Department of Earth & Environment, Boston University
[4]Department of Geology and Geophysics, Yale University

Stochastic atmospheric forcing and ENSO flavors: When it comes to ENSO predictability many studies have exploited precursor dynamics in the ocean and atmosphere that lead to mature expressions of El Niño. These include dynamics associated with westerly wind bursts (WWB) with El Niño lead times on the order of half-a-year or longer (McPhaden 1999; McPhaden and Yu 1999; Fedorov 2002), and with extra-tropical wind forcing (ETWF) via the "seasonal foot-printing mechanism" (SFM; Vimont et al. 2001; Vimont et al. 2003) and the "trade wind charging" (TWC) mechanism (Anderson 2003; Anderson et al. 2013a), with lead times of ~12 months. The WWB, SFM, and TWC precursor dynamics have their origin in stochastic atmospheric variability and have been linked to stochastic excitations of ENSO (Moore and Kleeman 1999; Penland and Sardeshmukh 1995). While previous studies have explored these precursor dynamics in the context of the "canonical" or eastern Pacific El Niño, the recognition that El Niño events have different flavors like the central Pacific El Niño (Ashok et al. 2007), has opened a new discussion within the U.S. CLIVAR ENSO Diversity Working Group on the role of these precursor dynamics in energizing the different flavors of El Niño or more generally the ENSO continuum.

The WWB precursor dynamics occur in the equatorial Pacific near the Dateline where intraseasonal atmospheric variability can generate zonal wind anomalies that excite eastward propagating equatorial Kelvin waves, which in turn favor the development of El Niño by deepening the thermocline, reducing upwelling and initiating the Bjerknes feedback. Although this mechanistic link between WWB and ENSO is sometimes difficult to establish in observations, numerical simulations show that a WWB can lead to an Eastern Pacific El Niño (Lengaigne et al. 2004) if the ocean state is recharged (heat content is higher than normal). However, a more recent numerical study shows that if the ocean state is in neutral conditions the WWB lead to a central Pacific El Niño (Fedorov et al. 2013). This latter study was conducted using two sets of ensemble experiments. In the first set, the initial ocean heat content of the system is higher than the model climatology (or recharged), while in the second set it is nearly normal (neutral). For the recharged state, in the absence of WWBs, a moderate central Pacific El Niño (CP) develops in about a year. In contrast, for the neutral state, there develops a weak La Niña. However, when the WWB is imposed, the situation dramatically changes: the recharged state slides into an eastern Pacific El Niño (EP), possibly of an extreme amplitude, while the neutral set shifts into a weak CP El Niño instead of previous La Niña conditions. The different response of the system to the exact same perturbations is controlled by the initial state of the ocean and the subsequent ocean-atmosphere interactions involving the interplay between the warming of the eastern equatorial Pacific and the eastward shift of the warm pool. In this